

## Environmentally Friendly Expeditious One-Pot Electrochemical Synthesis of Bis-Catechol-Thioether Metabolites of Ecstasy: *in vitro* Neurotoxic Effects in the Rat Hippocampus

Anne Felim<sup>1</sup>, Anne Neudörffer<sup>1</sup>, François P. Monnet<sup>2</sup> and Martine LARGERON<sup>1,\*</sup>

<sup>1</sup> UMR 8638 CNRS - Université Paris Descartes, Synthèse et Structure de Molécules d'Intérêt Pharmacologique, Faculté des Sciences Pharmaceutiques et Biologiques, 4 Avenue de l'Observatoire, 75270 Paris Cedex 06, France

<sup>2</sup> U 705 INSERM/UMR 7157 CNRS- Universités Paris Descartes et Denis Diderot, Neuropsychopharmacologie des Addictions, Assistance Publique -Hôpitaux de Paris, Hôpital Fernand Widal, 200 rue du Faubourg Saint-Denis, 75475 Paris Cedex 10, France.

\*E-mail: [martine.largeron@univ-paris5.fr](mailto:martine.largeron@univ-paris5.fr)

Received: 6 November 2007 / Accepted: 27 December 2007 / Online published: 20 January 2008

---

A straightforward one-pot electrochemical synthesis of bis-catechol-thioether metabolites of MDMA (ecstasy), 2,5-bis(glutathion-*S*-yl)-*N*-methyl- $\alpha$ -methyldopamine and 2,5-bis(*N*-acetylcystein-*S*-yl)-*N*-methyl- $\alpha$ -methyldopamine, in acceptable yields and high degree of purity (99%), is described under environmentally friendly conditions. The undeniable benefits of this method, which uses *N*-methyl- $\alpha$ -methyldopamine as the starting catechol, without the need to isolate the catechol-thioether mono-conjugate intermediate, include atom economy, as well as economies of time, resource management, and waste generation. Finally, the possible participation of the catechol-thioether bis-conjugates in the long-term neurotoxic effects of MDMA is discussed through their ability to elicit necrosis and apoptosis on rat hippocampal pyramidal neurons.

---

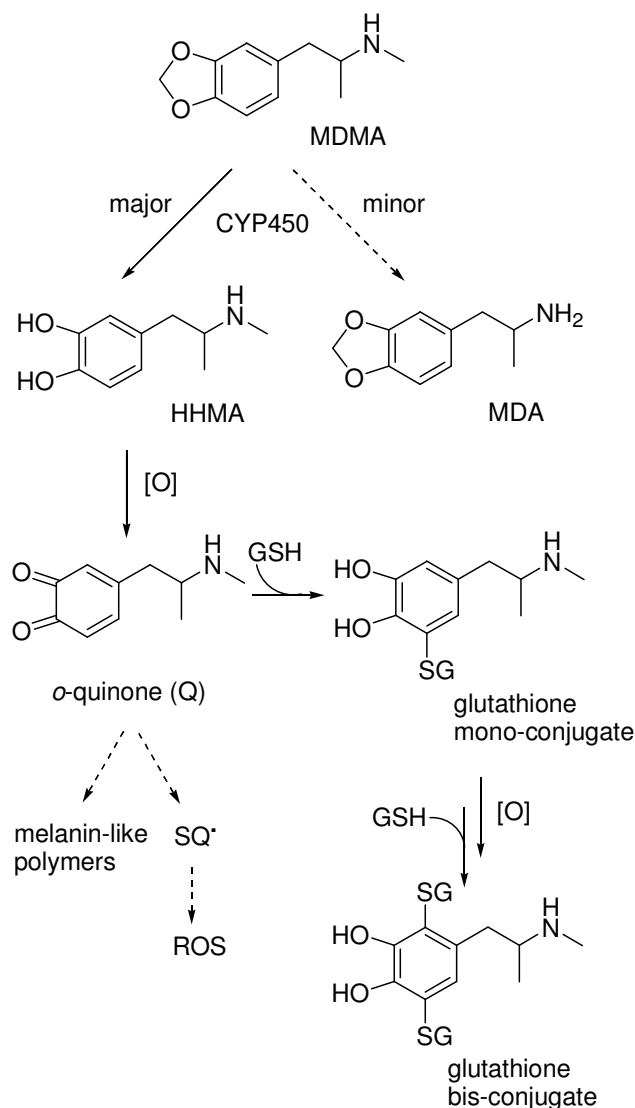
**Keywords:** anodic oxidation, ecstasy, *in vitro* neurotoxicity, quinone, thioether metabolites

### 1. INTRODUCTION

Over the past 20 years, ( $\pm$ )-3,4-methylenedioxymethamphetamine (MDMA, also known as “ecstasy”), has gained great popularity as a recreational drug, mainly among young people, due to its stimulant and hallucinogenic properties [1,2]. However, there are many concerns over its short-term and long-term effects. First, abuse of MDMA is associated with the risk of severe, sometimes fatal, intoxication [3-5]. Second, there is considerable evidence to indicate that MDMA has neurotoxic potential toward brain serotonergic and/or dopaminergic nerve terminals [6-9]. Consequently,

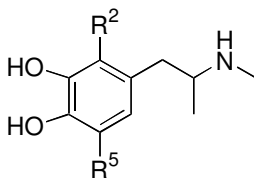
prospective clinical studies involving MDMA administration to humans are constrained by ethical considerations, so that only post-mortem studies might be performed. This justifies the extensive use of experimental model animals for the examination of the long-term effects of MDMA [10].

The idea of neurotoxic metabolites of MDMA is now well established [11] and originates from the finding that direct injection of the drug into specific brain areas (especially cortex, hippocampus and striatum) of the rat fails to reproduce the neurotoxic effects seen after systemic MDMA administration [12], and the report that alteration of cytochrom P450-mediated MDMA metabolism influences MDMA-induced neurotoxicity [13]. Nevertheless, the exact identity and the mechanism by which these metabolites initiate and propagate the neurotoxic events remain to be thoroughly established.



**Scheme 1.** Proposed routes for MDMA metabolism in humans leading to redox active catechol-thioether conjugates

MDMA metabolism proceeds via two pathways, which operate in unison but at different rates, depending on species [6, 11]. In humans, MDMA is essentially metabolized, through *O*-demethylenation, into 3,4-dihydroxymethamphetamine (HHMA), whereas *N*-demethylation leading to 3,4-methylenedioxyamphetamine (MDA) constitutes a minor metabolic route (Scheme 1) [14]. Because of its catechol moiety, HHMA can be easily oxidized to the corresponding *o*-quinone species which exhibits a double reactivity. First, it can undergo redox-cycling which originates semiquinone radical and leads to the generation of reactive oxygen species (ROS). Second, it behaves as a highly electrophilic compound which can be conjugated with thiol nucleophiles such as glutathione (GSH), to form the 5-(glutathion-*S*-yl) mono-conjugate. This GSH conjugate remains redox-active, being readily oxidized to the corresponding *o*-quinone-thioether species, which can, in its turn, undergo either redox-cycling or further reaction with thiols, affording the redox-active 2,5-bis(glutathion-*S*-yl) conjugate.



- HHMA :  $R^2 = R^5 = H$   
**1** :  $R^2 = H$ ;  $R^5 = \text{glutathion-}S\text{-yl}$   
**2** :  $R^2 = H$ ;  $R^5 = \text{N-acetylcystein-}S\text{-yl}$   
**3** :  $R^2 = R^5 = \text{glutathion-}S\text{-yl}$   
**4** :  $R^2 = R^5 = \text{N-acetylcystein-}S\text{-yl}$

**Chart 1.** Structural formulae of HHMA and catechol-thioether conjugates **1-4**

Taken together, MDMA-metabolism leading to the formation of ROS and/or toxic oxidation products, may represent the triggering factors responsible for MDMA-induced neurotoxicity. Evidently, whether or not the catechol-thioether metabolites are involved in MDMA-mediated neurotoxicity would depend upon their ability to cross the blood-brain barrier. In this respect, recent investigations have shown that GSH and N-acetylcysteine (NAC) mono-conjugates **1** and **2** (Chart 1) are present in the striatum of rats, following MDMA subcutaneous injection [15]. Furthermore, as multi-dose administration of MDMA is typical of drug intake during rave parties, effects of multiple doses of MDMA on the concentration of catechol-thioether metabolites in rat brain have been analyzed. The data indicate that neurotoxic metabolites of MDMA, especially the 2,5-bis-NAC conjugate, may accumulate in brain following multiple dosing [16]. All these results would indicate that MDMA and HHMA do not appear in the brain in their free form but rather are transported in their conjugate form from the periphery. In addition, at least one of these metabolites, 5-(*N*-acetylcystein-*S*-yl)-*N*-methyl- $\alpha$ -methyldopamine **2** produces serotonergic neurotoxicity when injected directly into the rat striatum [15]. To date, additional experiments are again necessary to undoubtedly establish the

participation of the catechol-thioether mono- and bis-conjugates in the *in vivo* neurotoxic effects of the drug. Unfortunately, these conjugates are not easily accessible stable compounds, so that their synthesis has received scant attention.

To the best of our knowledge, only an enzymatic procedure involving the oxidation of HHMA with mushroom tyrosinase, in the presence of GSH or NAC, has been reported for the synthesis of the catechol-thioether mono-conjugates **1** and **2**, respectively [15, 17]. However the enzymatic procedure is not adapted for routine syntheses, because it is too expensive and not suitable for yielding substantial amounts of conjugates. Concerning the synthesis of bis-conjugates **3** and **4**, resulting from two consecutive 1,6-Michael addition reaction of thiol, a sole method using sodium periodate as the oxidizing agent in aqueous solution of 10% formic acid has been described (yield not given) [16].

For a long time, electrochemical oxidation has proved to be an efficient tool for the generation of highly electrophilic quinones species, which can be further scavenged by diverse nucleophilic entities such as thiol groups. Accordingly, unstable *o*-quinone species have been electrogenerated from catechols [18,19], and catecholamines such as dopamine [20-23] norepinephrine [24] or *N*-acetyldopamine [25], and then scavenged by thiol residues to afford the corresponding catechol-thioether adducts.

As part of our ongoing program devoted to the reactivity of quinonoid systems with nucleophiles closely related to biological processes [26-30], we recently reported a detailed electrochemical methodology allowing the straightforward one-pot synthesis of diverse catechol-thioether mono-conjugates of MDMA, resulting from the addition of GSH, NAC or cysteine, in good yields ( $\approx 60\%$ ) and high degree of purity (99%) [31]. Then, we decided to adapt our aforementioned electrochemical method to the synthesis of bis-conjugates **3** and **4**, using catechol-thioether mono-conjugates **1** and **2** as the starting materials, respectively. Surprisingly, our initial attempts to prepare the expected products were disappointing, leading to low yield of the desired bis-conjugates (21% for **3** and 10% for **4**). At this point, we questioned about the reasons for such results, in order to propose a convenient alternative synthetic route.

In this paper, we report a full account of the electrochemical methodology allowing the expeditious one-pot synthesis of catechol-thioether bis-conjugates **3** and **4** (Chart 1), in acceptable yields and high degree of purity (99%), using HHMA as the starting material, without the need to isolate the mono-conjugate intermediate. Furthermore, the possible implication of the catechol-thioether bis-conjugates **3** and **4** in the long-term neurotoxicity of MDMA has been estimated *in vitro* through their capacity to elicit necrosis and apoptosis on rat hippocampal pyramidal neurons. The results have been compared with those of MDMA, HHMA, and the corresponding mono-conjugates **1** and **2** evaluated in the same test system.

## 2. MATERIALS AND METHODS

### 2.1. Chemistry

All reagents and solvents (HPLC grade) were commercial products of the highest available purity, and were used as supplied. ( $\pm$ )-*N*-methyl- $\alpha$ -methyl-dopamine hydrobromide was synthesized in

four steps, from commercially available 3,4-dimethoxy-benzaldehyde and nitroethane, through procedures previously reported [32-35]. 5-(Glutathion-S-yl)-*N*-methyl- $\alpha$ -methyldopamine **1** and 5-(*N*-acetylcystein-S-yl)-*N*-methyl- $\alpha$ -methyldopamine **2** were synthesized through our recently reported one-pot electrochemical procedure [31].

HPLC was carried out using a Waters system, consisting of a 600E multisolvent delivery system, a Rheodyne-type loop injector, and a 2487 dual-channels UV-visible detector set at 254 and 278 nm. A mixture of three solvents constituted the mobile phase: acetonitrile (MeCN), solvents A and B. Solvent A was prepared by adding 1% concentrated trifluoroacetic acid (TFA) to deionized water. Solvent B was prepared by adding 0.5% TFA to a mixture of equivalent volumes of deionized water and methanol. Semi-preparative reversed-phase HPLC was performed using a 250 x 20 mm – 5  $\mu$ m-Kromasil C18 column and a 2 mL loop injector, while, for analytical reversed-phase HPLC, a 250 x 4.6 mm - 5  $\mu$ m- Kromasil C18 column, together with a 50  $\mu$ L loop injector, were used.

## 2.2. Electrochemistry

Electrochemical measurements were made with a Radiometer-Tacussel PRG 5 multipurpose polarograph, which was used only as a rapid-response potentiostat. For cyclic voltammetry, triangular waveforms were supplied by a Tacussel GSTP 4 function generator. Current-potential curves were recorded on a Schlumberger SI 8312 instrument. The cell was a Radiometer-Tacussel CPRA water-jacketed cell working at a temperature of 25°C. The working electrode was a platinum disk, carefully polished before each voltammogram with an aqueous alumina suspension. The counter electrode was a platinum electrode Tacussel Pt 11. The reference electrode was an Ag/AgCl electrode, to which all potentials quoted are referred.

Controlled-potential electrolyses were carried out using a DEA 332 electrochemical analyzer (Radiometer, Copenhagen), in a cylindrical three-electrode divided cell (9 cm diameter). In the main compartment, a cylindrical platinum grid (area = 60 cm<sup>2</sup>) served as the anode (working electrode). A platinum sheet was placed in the concentric cathodic compartment (counter-electrode), which was separated from the main compartment with a glass frit. The reference electrode was as above described.

### 2,5-bis(glutathion-S-yl)-*N*-methyl- $\alpha$ -methyl-dopamine (**3**)

*Procedure A.* A solution of 5-(glutathion-S-yl)-*N*-methyl- $\alpha$ -methyldopamine (**1**) (121.5 mg, 0.25 mmol), in 0.2 M HCl (250 mL), was oxidized under nitrogen, at room temperature, at a platinum grid whose potential was fixed at + 1.0 V versus Ag/AgCl. After the consumption of 2 electrons per molecule, 2 equiv of glutathione (157 mg, 0.50 mmol) were added to the reaction mixture, which was immediately frozen at – 80°C and then freeze-dried. The residue was subdivided in fractions of about 25 mg. Each fraction was dissolved in 2 mL of water and then purified by semi-preparative reversed-

phase HPLC, using a mixture of solvent A/ solvent B 72/28 as the eluent (flow rate: 3 mL min<sup>-1</sup>). Fractions containing 2,5-bis(glutathion-*S*-yl)-*N*-methyl- $\alpha$ -methyldopamine (**3**) and 5-(glutathion-*S*-yl)-*N*-methyl- $\alpha$ -methyldopamine (**1**) were collected individually, immediately frozen at -80°C, and then freeze-dried. Compound **3** was isolated as the major product in 21% yield (pale pink solid, 42 mg, 0.05 mmol). The degree of purity for compound **3** (99%) was determined by analytical HPLC (eluent: solvent A/ MeCN 94/6 – flow rate: 0.8 mL min<sup>-1</sup>). In 0.2 M HCl, compound **3** exhibited a UV band at 274 nm ( $\epsilon = 7200 \text{ mol}^{-1} \text{ L cm}^{-1}$ ) and a shoulder at 305 nm. <sup>1</sup>H NMR, <sup>13</sup>C NMR and mass spectroscopic data were identical to those previously reported [31].

*Procedure B.* A solution of 5-(glutathion-*S*-yl)-*N*-methyl- $\alpha$ -methyldopamine (**1**) (121.5 mg, 0.25 mmol), in 0.2 M HCl (250 mL), was oxidized under nitrogen, at room temperature, at a platinum grid whose potential was fixed at + 1.0 V versus Ag/AgCl, in the presence of 2 equiv of glutathione (157 mg, 0.50 mmol). After the consumption of 2 electrons per molecule, the electrolysis was stopped and 2 equiv of glutathione (157 mg, 0.50 mmol) were added to the reaction mixture, which was immediately frozen at -80°C and then freeze-dried. The residue was then treated as above mentioned. Compound **3** was isolated as the major product in 54% yield (pale pink solid, 107 mg, 0.135 mmol), along with compound **1** as the minor one, in 7% yield (8.5 mg, 0.017 mmol).

*Procedure C:* A solution of ( $\pm$ )-*N*-methyl- $\alpha$ -methyldopamine hydrobromide (65.5 mg, 0.25 mmol) in 0.2 M hydrochloric acid (250 mL) was oxidized under nitrogen, at room temperature, at a platinum grid ( $E = + 1.0 \text{ V}$  versus Ag/AgCl). After the consumption of 2 electrons per molecule, the electrolysis was stopped and 3 equiv of glutathione (235 mg, 0.75 mmol) were added. When the yellow electrolysis solution became colorless, it was oxidized again at + 1.0 V versus Ag/AgCl. After exhaustive electrolysis ( $n = 5.8$ , that is 2.0 for the first step and 3.8 for the second one), 2 equiv of glutathione (157 mg, 0.50 mmol) were added to the reaction mixture, which was immediately frozen at -80°C, and then freeze-dried. The residue was then treated as above mentioned. Compound **3** was isolated as the major product in 50% yield (99 mg, 0.13 mmol), along with compound **1** in 22% yield (26.5 mg, 0.055 mmol).

#### *2,5-bis(N-acetylcystein-S-yl)-N-methyl- $\alpha$ -methyl-dopamine (4)*

The procedure C, replacing glutathione by *N*-acetylcysteine (208 mg, 1.25 mmol, overall quantity), afforded, after exhaustive electrolysis ( $n = 5.5$ , that is 2 for the first step and 3.5 for the second one) and semi-preparative reversed-phase HPLC (eluent: solvent A/ solvent B 93/17 - flow rate: 14 mL min<sup>-1</sup>), 2,5-bis(*N*-acetylcystein-*S*-yl)-*N*-methyl- $\alpha$ -methyldopamine (**4**), in 44% yield (white solid, 55 mg, 0.11 mmol), along with compound **2**, in 22% yield (19 mg, 0.055 mmol). The degree of purity for compound **4** (99%) was determined by analytical HPLC (eluent: solvent A/ MeCN 92/8 – flow rate: 0.8 mL min<sup>-1</sup>). In 0.2 M HCl, compound **4** exhibited UV bands at 274 nm ( $\epsilon = 6390 \text{ mol}^{-1} \text{ L cm}^{-1}$ ) and a shoulder at 305 nm. <sup>1</sup>H NMR, <sup>13</sup>C NMR and mass spectroscopic data were identical to those previously reported [31].

### 2.3. Biological investigations.

#### 2.3.1. Primary hippocampal neuronal culture and experimental treatments.

The classical procedure for obtaining a homogeneous culture of nearly pure hippocampal pyramidal neurons was utilized [36]. Under these conditions, more than 95 % of the cells are neurons as evaluated using  $\alpha$ -tubulin and glial fibrillary acidic protein (GFAP) immunoreactivity (data not shown). Such purity is obtained from the use of hippocampi at embryonic day 18 (ED18), which avoids the inclusion of dentate gyros granular neurons which develop from ED21. The elimination of serum from the culture medium, which is not propitious to glial cell proliferation, was also mandatory to get low rate of GFAP-positive cells. Hippocampal formation from ED18 Sprague-Dawley embryo rats was isolated after careful removal of the pia mater and then mechanically dissociated by triturating and pipetting up and down with fire-polished sterile Pasteur pipettes in  $\text{Ca}^{++}$ - and  $\text{Mg}^{++}$ -free Krebs buffer (NaCl 118, KCl 5,  $\text{NaH}_2\text{PO}_4$  1.2,  $\text{NaHCO}_3$  20, glucose 16, Hepes 10). After dissociation, the cells were centrifuged once (1000 rpm for 10 min, 4°C) to remove cellular debris, and cells were then plated onto sterile 25 mm-diameter poly-L-ornithine (1.5  $\mu\text{g}/\text{mL}$ )-coated culture glass coverslips (Menzel-Gläser, Braunschweig, Germany), at a density of  $\approx 10^6$  cells/mL, seeded into 6-well (Falcon, Becton-Dickinson Labware, Franklin Lakes, NJ, USA) plates of 30-mm diameter with 1.5 mL buffer. Hippocampal cells were grown in Dulbecco's modified Eagle's medium (DMEM, Gibco-BRL, Gaithersburg, MD, USA), supplemented with 2 mM L-glutamine,  $6 \times 10^{-5}$  M putrescine, 25  $\mu\text{g}/\text{mL}$  insulin, 20 U/mL penicillin, 0.02 mg/mL streptomycin, 2.5 mM HEPES,  $3 \times 10^{-8}$  M selenium, 0.6 % glucose, 100  $\mu\text{g}/\text{mL}$  apotransferrin, and maintained in a humidified incubator with 5%  $\text{CO}_2$ , at 37 °C, for 5 to 7 days prior to immunohistochemical staining. One hour prior to seeding, the glass coverslips were rinsed once with foetal calf serum (10 %) supplemented DMEM. The culture medium was changed by half each two days.

#### 2.3.2. Examination of the neuronal viability in the rat hippocampus

After two days of incubation, MDMA, HHMA, together with catechol-thioethers conjugates **1-4** were added to hippocampal pyramidal neurons for 48/72 hours. At this time, neuronal injury was assessed by analysis of the cellular/nuclear morphology by fluorescence microscopy of live cells using the stains propidium iodide and Hoechst-33342 which enter the cells only when membrane integrity is lost and fluoresce red and blue, respectively. After washing, hippocampal cells on the glass coverslips were fixed with formaldehyde (4 %, 10 min) and permeabilized with Triton-X 100 (0.1 %, 5 min). Viable, necrotic and apoptotic neurons were visualized by nuclear morphology criteria. Viable cells display a normal nuclear size and homogeneous fluorescence. Necrotic neurons manifest fluorescence without chromatin condensation. Apoptotic neurons include cells that display pyknotic nuclei with condensed or fragmented chromatin. Cells were examined and scored with a Nikon EZ-C1 microscope (Champigny/Marne, France). The excitation light was supplied by a high pressure xenon arc lamp (100 W). All experiments were performed in triplicate from at least four cultures, and a minimum of 200

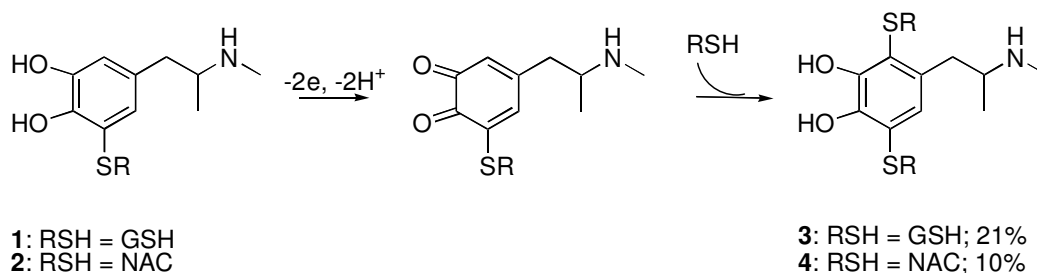
cells were scored for each coverslip. The number of viable, necrotic and apoptotic neurons was expressed as the percentage of the total number of cells in the microscope field.

### 3. RESULTS AND DISCUSSION

#### 3.1. Chemical Investigations

##### 3.1.1. Electrochemical synthesis of 2,5-bis(glutathion-S-yl) conjugate **3**

At the outset, we decided to adapt our electrochemical procedure, previously described for the preparation of mono-conjugate **1**, to the synthesis of bis-conjugate **3**, using catechol-thioether mono-conjugate **1** as the starting material [31]. So, the anodic oxidation of mono-conjugate **1** was conducted in the absence of glutathione, under acidic conditions. Subsequent addition of glutathione to the electrogenerated *o*-quinone-thioether species should afford the desired catechol-thioether bis-conjugate **3** as shown in scheme 2.



**Scheme 2.** Two-step one-pot electrochemical synthesis of catechol-thioether bis-conjugates **3** and **4**, using catechol-thioether mono-conjugates **1** and **2** as the starting materials, respectively.

Accordingly, the cyclic voltammogram of mono-conjugate **1** (1 mM), in deaerated 0.2M HCl aqueous solution, at room temperature, showed, at a platinum anode, an oxidation peak Pa at + 560 mV versus Ag/AgCl, due to a two-electron process, the sweep rate being 10 mV s<sup>-1</sup>. As can be seen in Figure 1, a cathodic peak Pc appeared on the reverse sweep at 440 mV versus Ag/AgCl, illustrating the quasireversibility of the two-electron transfer that could be assigned to the *o*-quinol-thioether/*o*-quinone-thioether redox couple. However, the redox potential  $E'^{\circ}$  could not be accurately evaluated under our experimental conditions, as the system (Pa, Pc) did not fulfil all the diagnostic criteria required for a reversible process, at least when  $v$  was  $\leq 200$  V s<sup>-1</sup>: the ratio of the height of Pa over that of Pc never reached unity ( $i_{Pc}/i_{Pa} \approx 0.7$ ) and the value of  $E_{Pa} - E_{Pc}$  ( $E$  being the peak potential) was found to be higher than 30 mV. Although mono-conjugate **1** and HHMA were oxidizable at similar potential (Figure 1), the reversibility of the process was lower in the case of mono-conjugate **1**, indicating that the produced *o*-quinone-thioether species was partly engaged in a follow-up reaction even at the time scale of cyclic voltammetry.



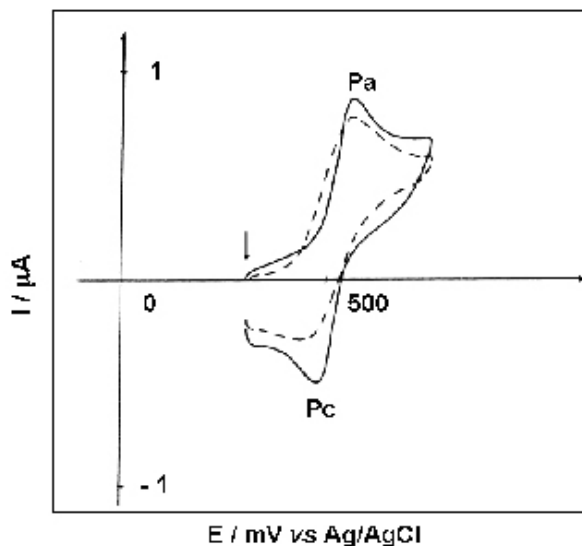


**Figure 1.** Cyclic Voltammogram of HHMA (solid line) and 5-glutathion-S-yl mono-conjugate **1** (dashed line) (1 mM), at a platinum electrode in deaerated 0.2 M HCl aqueous solution,  $v = 10 \text{ mVs}^{-1}$ . The vertical arrow indicates the initial potential point.

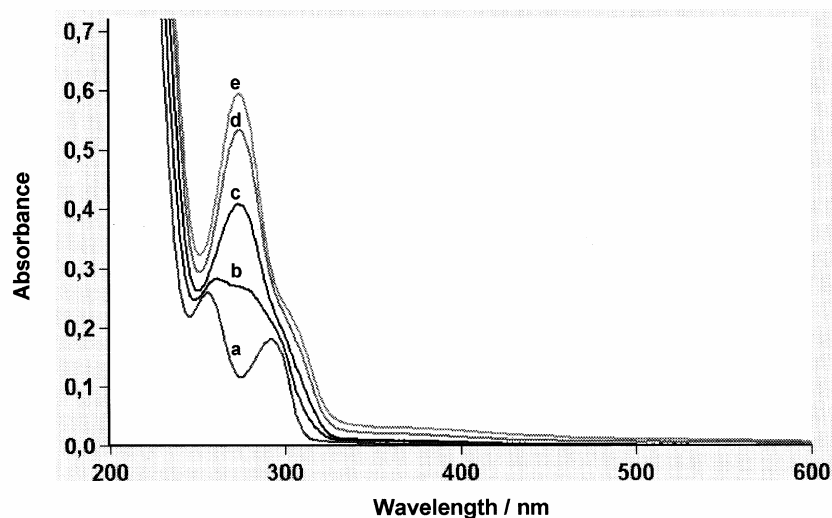


**Figure 2.** Spectrophotometric changes accompanying the electrochemical oxidation of 5-glutathion-S-yl mono-conjugate **1** (1mM), at a platinum anode ( $E = + 1.0 \text{ V}$  versus Ag/AgCl), in deaerated 0.2 M HCl aqueous solution in the presence of glutathione (2mM): (a) 0 (before electrolysis), (b) 0.5, (c) 1.0, (d) 1.5, and (e) 2.0 mol of electrons. Cell thickness is 0.1 cm.

When the controlled potential of the platinum anode was fixed at + 1.0 V versus Ag/AgCl, which is at a potential following the anodic peak observed in cyclic voltammetry, the electrolysis solution rapidly became dark purple, in agreement with the instability of the electrogenerated *o*-

quinone-thioether species. This was substantiated by monitoring the UV-vis absorption spectrum in the course of the electrolysis. After applying the potential, a significant decrease in the UV-vis absorption band at 256 nm ( $\epsilon = 2580 \text{ mol}^{-1} \text{ L cm}^{-1}$ ) and 292 nm ( $\epsilon = 1800 \text{ mol}^{-1} \text{ L cm}^{-1}$ ) shown by the mono-conjugate **1** was observed. Contrary to what has been observed for the electrochemical oxidation of HHMA which produced a rather stable *o*-quinone species (see figure 3 below, spectra a-e), spectral changes did not show isosbestic points. No definite UV-vis absorption spectrum was recorded at the end of the electrolysis indicating the partial decomposition of the electrogenerated *o*-quinone-thioether species. Accordingly, subsequent addition of 2 equiv of thiol derivative did not result in the discoloration of the dark purple solution, in agreement with the formation of melanin-like polymers. Treatment of the electrolysis solution afforded, after semi-preparative reversed-phase HPLC (See Experimental Section), 2,5-bis-catechol-thioether conjugate **3**, in only 21% yield. This result confirmed the high instability of the quinone-thioether species in the course of the electrolysis process.

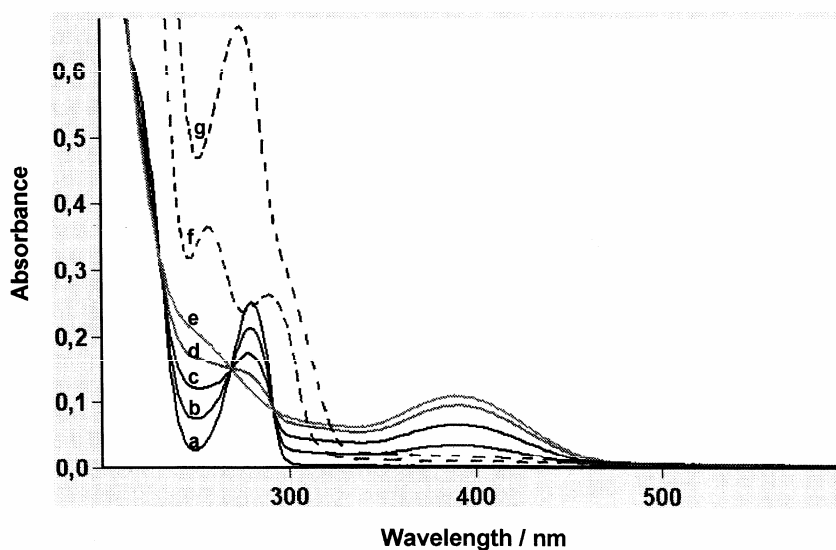
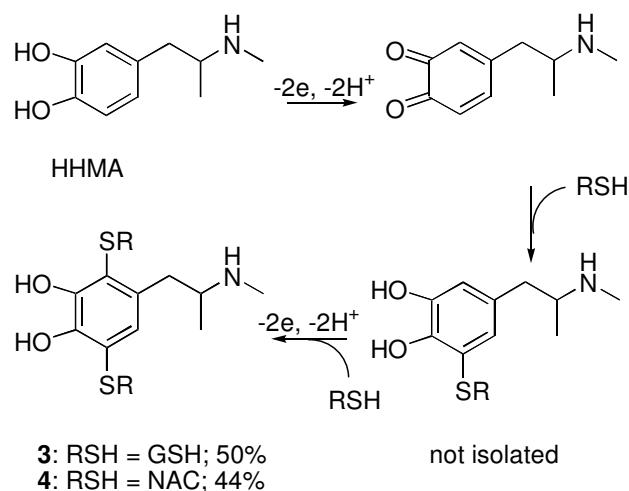


**Figure 3.** Spectrophotometric changes accompanying the multi-step one-pot electrosynthesis of 2,5-(glutathion-*S*-yl) bis-conjugate **3**. (spectra a-e) : electrochemical oxidation of HHMA (1mM), at a platinum anode ( $E = + 1.0 \text{ V}$  versus Ag/AgCl), in deaerated 0.2 M HCl aqueous solution: (a) 0 (before electrolysis), (b) 0.5, (c) 1.0, (d) 1.5, and (e) 2.0 mol of electrons; (spectrum f): after addition of 2 equiv of glutathione to the two electrons-oxidized solution; (spectrum g): spectrum recorded after the consumption of additional 3.8 mol of electrons (end of the process). Cell thickness is 0.1 cm.

So, to circumvent this problem, we decided to oxidize the catechol-thioether mono-conjugate **1**, in the presence of glutathione. Then, we thought that the produced unstable *o*-quinone-thioether entity would be trapped by thiol derivative, before its decomposition. So, catechol-thioether conjugate **1** (1 mM) was oxidized in deaerated 0.2 M HCl aqueous solution, in the presence of 2 equiv of glutathione. When the potential of the platinum anode was fixed at + 1.0 V versus Ag/AgCl, which is at a potential for which **1** could be oxidized to the corresponding *o*-quinone-thioether species, a new band at 274 nm,

along with a shoulder around 300 nm, developed at the expense of both UV-vis absorption bands shown by **1** at 256 and 292 nm (Figure 2). This new spectrum could be assigned to the 2,5-bis-catechol-thioether conjugate **3**, as corroborated after recording the UV-vis absorption spectrum of the isolated product. Consequently, it could be deduced that the electrogenerated *o*-quinone-thioether intermediate was sufficiently reactive to be immediately engaged in subsequent 1,6-Michael addition reaction with glutathione. Treatment of the electrolysis solution afforded, after semi-preparative reversed-phase HPLC (See Experimental Section), catechol-thioether bi-adduct **3**, in 54% yield, along with 7% of the starting mono-adduct **1** (Chart 1). This result confirmed the higher instability of the *o*-quinone-thioether intermediate when compared with that of the *o*-quinone species.



**Scheme 3.** Multi-step one-pot electrochemical synthesis of catechol-thioether bis-conjugates **3** and **4**, using HHMA as the starting material.

In a second series of experiments aimed at simplifying the synthesis of the bis-catechol-thioether conjugate **3**, we envisioned a multi-step one-pot electrochemical procedure, which allowed the preparation of the bi-adduct, using HHMA as the starting material without the need to isolate the mono-adduct intermediate. Accordingly, the first part of the procedure consisted of the generation of the *o*-quinone species, using HHMA as the starting material, at a fixed potential of +1.0 V versus Ag/AgCl, under the aforementioned acidic conditions [31]. After the application of the potential, a decrease in the UV-vis absorption band shown by HHMA at 279 nm ( $\epsilon = 2360 \text{ mol}^{-1} \text{ L cm}^{-1}$ ) was observed, while a new band at 387 nm, along with a shoulder around 250 nm, developed. Spectral changes showed two isosbestic points at 268 and 290 nm, indicating that a simple equilibrium between two species was shifted (Figure 3, spectra a-e). As the electrogenerated *o*-quinone species was rather stable under these experimental conditions, subsequent addition of 2 equiv of thiol derivative resulted in the immediate discoloration of the yellow solution, indicating the formation of the catechol-thioether mono-conjugate **1**, which was evidenced by the change in the UV-vis absorption spectrum, showing new absorption maxima at 256 and 292 nm (Figure 3, spectrum f). In the second part of the procedure, after the electrolysis solution became colorless, a third equiv of glutathione was added, and

the resulting solution was oxidized again at + 1.0 V versus Ag/AgCl. Then, the solution became pale yellow and a coulometric value of 3.8 was found for n. No surprisingly, spectral changes were identical with those shown in figure 2. At the end of the electrolysis, the recorded spectrum g could be assigned to that of 2,5-bis-catechol-thioether conjugate **3**. To maintain a reducing medium during work-up, two additional equiv of glutathione were added. Finally, treatment of the electrolysis solution afforded, after semi-preparative reversed-phase HPLC (See Experimental Section), the catechol-thioether bi-adduct **3**, in 50% yield, together with 22% of the mono-adduct **1** (Scheme 3).

Interestingly, the overall yield of **3** (50%) was substantially improved following this multi-step one-pot method, since the classical two-step electrochemical synthesis would afford **3** in only 34% overall yield (64% for the first step corresponding to the synthesis of the mono-adduct intermediate **1** [31], and 54% for the second one leading to the bi-adduct **3** as above reported). Furthermore, the undeniable benefits of this electrochemical methodology also included atom economy, as well as economies of time, resource management, and waste generation since only one electrolysis, isolation and purification step were required.

### 3.1.2. Electrosynthesis of 2,5-bis(N-acetylcystein-S-yl) conjugate **4**

When applied to catechol-thioether mono-conjugate **2**, the aforementioned multi-step one-pot procedure, using HHMA as the starting material, allowed the isolation of 2,5-bis(N-acetylcystein-S-yl) conjugate **4**, in 44% yield, along with 22% of catechol-thioether conjugate **2**, isolated as a minor product (Scheme 3).

Note, in all cases, the presence of the catechol-thioether mono-conjugate as a minor product could not be avoided, probably because redox interchange occurred between the different redox systems present in the electrolysis solution. This point would merit thorough further mechanistic investigations.

### 3.2. Biological investigations

To rapidly examine the possible role of the catechol-thioether bis-conjugates **3** and **4** in the long-term neurotoxicity of MDMA, their effects on the cellular viability were assessed on rat pyramidal hippocampal neurons and compared with those shown by MDMA, HHMA and their related mono-conjugates **1** and **2** (Figure 4). The concentration of each tested compound was fixed at 10  $\mu$ M, because it spans the range of concentrations of MDMA seen in human one hour after a drug administration of a tablet [37]. This dosage is also clinically relevant since behavioral (anxiety, impulsive and aggressive behavior, mood fluctuation, empathy...) and biochemical effects occurred within the 2-40  $\mu$ M concentration range of MDMA, typically found in humans for recreational purposes [38]. However, this dosage remains a tenth to those reported for severe or fatal accidents.

The number of viable, necrotic and apoptotic hippocampal pyramidal neurons upon exposure to MDMA and its metabolites was analyzed by fluorescence microscopy after propidium iodide/Hoechst-33342 labelling (See Experimental). Exposure of pyramidal neurons to MDMA (10  $\mu$ M) did not reveal

any modification in the number of viable, necrotic and apoptotic cells after 48/72h of incubation with the control situation (Figure 4). Note that the time of incubation corresponded to the optimal delay for observing the maximum hippocampal abnormalities [39]. So, as previously reported [12], MDMA (10  $\mu$ M/48-72h) was not cytotoxic for hippocampal pyramidal neurons. This result supported the statement that MDMA might be toxic via its metabolites [11,12,15,35].

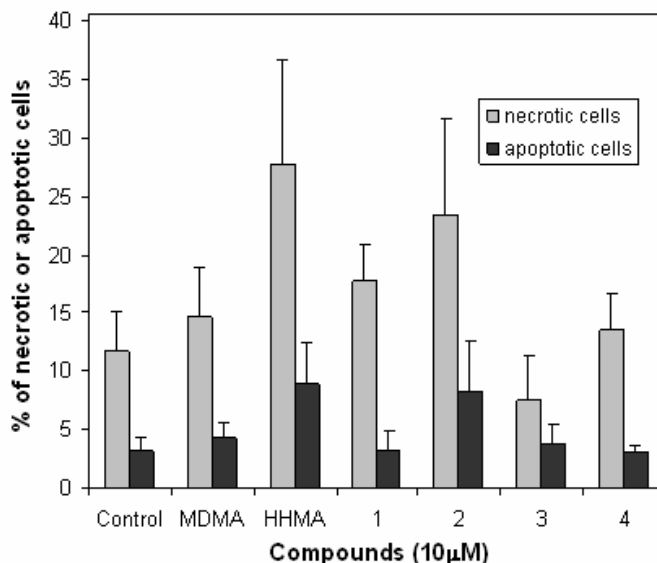


**Figure 4.** Drug dependent variations of neuronal viability from primary culture of rat hippocampal neurons. The necrotic and apoptotic status of the pyramidal neurons were assessed from 5-7 days in culture, after 48/72 hours with MDMA, HHMA and catechol-thioether conjugates **1-4**. Propidium iodide and Hoechst-33342 were used to identify cell permeant neurons, pyknotic nuclei and chromatin condensation. Necrotic neurons manifest fluorescence without chromatin condensation. Apoptotic neurons display pyknotic nuclei with condensed or fragmented chromatin. Each value represents the mean  $\pm$  SEM of at least ten microscopic fields from at least four independent cultures.

Accordingly, we found that the most efficient metabolites to affect cell viability after 48-72h were HHMA and 5-*N*-acetylcystein-*S*-yl mono-conjugate **2** (Figure 4). Treatment of hippocampal neurons with either HHMA [35] or **2** increased the number of necrotic cells and enhanced the number of neurons exhibiting apoptotic morphology. In contrast, with 5-glutathion-*S*-yl mono-conjugate **1**, the number of apoptotic cells was not significantly affected upon treatment of hippocampal neurons, while the number of neurons exhibiting necrotic morphology slightly increased. Similarly, incubation with the catechol-thioether bis-conjugates **3** and **4** did not produce any further necrosis and apoptosis when compared to the control situation (Figure 4). Interestingly, these results confirmed that the catechol-thioether bis-conjugates **3** and **4** were less toxic than the parent mono-conjugates **1** and **2**, in accordance with our own results obtained from *Escherichia coli* plate assays [31] and with other results previously obtained on rat cortical neurons [40]. Furthermore, *N*-acetylcystein-*S*-yl conjugate **2** was found the most potent neurotoxicant, as previously reported [15].

#### 4. CONCLUSIONS

Despite several years of intensive efforts, the mechanisms by which MDMA produces long-term damage to serotonin and/or dopamine nerve endings remain to be fully elucidated. In particular, the sequence order of events and the identity of a specific neurotoxic entity (if there is only one) have yet to be determined. However, systemic formation of catechol-thioether metabolites *in vivo* [15] and the complex array of polymorphic enzymes that participate in their formation offer a new perspective for MDMA-induced neurotoxicity.

This prompted us to develop a straightforward multi-step one-pot electrochemical synthesis of catechol-thioether bis-conjugates of MDMA **3** and **4**, which proved to be especially attractive for routine synthesis, with acceptable yields, high degree of purity (99%) and environmentally friendly conditions. The utilization of electricity as energy instead of oxidative reagents, aqueous media instead of organic solvents, room temperature, one-pot operation and high atom economy, are of preeminent green advantages. To the best of our knowledge, at the exclusion of a synthesis which used the mono-conjugate as the starting material, and sodium periodate as the oxidizing agent (yield not given) [16], these catechol-thioether bis-conjugates have never been prepared as yet.

To gain insight into the possible participation of the catechol-thioether bis-conjugates **3** and **4** in the neurotoxic events of MDMA, we have examined their capacity to elicit necrosis and apoptosis on rat hippocampal pyramidal neurons, in comparison with that exhibited by MDMA, HHMA and related mono-conjugates **1** and **2**. Our results confirmed that MDMA itself is not neurotoxic over a 48/72h period as previously shown [12]. In this respect, the lack of neurotoxicity following local application of MDMA in the hippocampus suggests that MDMA-induced neurotoxicity would not be due to the parent compound, and that an active peripheral metabolite is responsible for the neuronal damage. Nevertheless, the identification of the most relevant toxic metabolite is not easy.

From the present *in vitro* results, catechol-thioether mono-conjugate **2** was found to be the most toxic metabolite of the studied series, while the catechol-thioether bis-conjugates **3** and **4** (10  $\mu$ M) did not produce significant necrosis and apoptosis. However, it is important to note that it has recently been shown that catechol-thioether bis-conjugates, **4** especially, may accumulate in brain following multi-dose administration of MDMA [16], which is typical of drug intake during rave parties. Consequently, although less toxic than the related mono-conjugates **1** and **2**, the possible participation of the catechol-thioether bis-conjugates **3** and **4** in the neurotoxic events of MDMA proved to be plausible.

Finally, the last question that remains is the relevance of our *in vitro* results to the *in vivo* situation because other pathways could also contribute to overall MDMA toxicity. In this respect, the new electrochemical methodology we describe should permit, thanks to the preparation of noticeable quantities, a comprehensive examination, both *in vitro* and *in vivo*, of the exact role of the catechol-thioether metabolites **1-4** in the neurotoxic effects of ecstasy.

#### ACKNOWLEDGEMENTS

We thank Dr. M.-B. Fleury, Emeritus Professor, Paris Descartes University, for helpful discussions. This Research was made possible thanks to the joint financial support of the Mission Interministérielle

de Lutte contre la Drogue et la Toxicomanie (MILDT) and the Institut National de la Santé et de la Recherche Médicale (INSERM). (Appel à projets commun 2004 MILDT-INSERM « Recherche sur les drogues et la toxicomanie »). A.F. thanks MILDT together with INSERM for a PhD grant.

## References

1. R.H. Schwartz, N.S. Miller, *Pediatrics* 100 (1997) 705.
2. K.M. Hegadoren, G.B. Baker, M. Bourin, *Neurosci. Biobehav. Rev.* 23 (1999) 539.
3. C.M. Milroy, J.C. Clark, A.R.W. Forrest, *J. Clin. Pathol.* 49 (1996) 149.
4. A. Walubo, D. Seger, *Hum. Exp. Toxicol.* 18 (1999) 119.
5. V. Fineschi, F. Centini, E. Mazzeo, E. Turillazzi, *Forensic Sci. Int.* 104 (1999) 65.
6. A.R. Green, A.O. Mehan, J.M. Elliot, E. O'Shea, M.I. Colado, *Pharmacol. Rev.* 55 (2003) 463 and references therein.
7. J. Lyles, J.L. Cadet, *Brain Res. Rev.* 42 (2003) 155 and references therein.
8. J. Morton, *Curr. Opinion Pharmacol.* 5 (2005) 79.
9. G.A. Ricaurte, U.D. McCann, *Lancet* 365 (2005) 2137.
10. N. Easton, C.A. Marsden, *J. Psychopharmacol.* 20 (2006) 194 and references therein.
11. T.J. Monks, D.C. Jones, F. Bai, S.S. Lau, *Ther. Drug Monit.* 26 (2004) 132 and references therein.
12. B. Esteban, E. O'Shea, J. Camarero, V. Sanchez, A.R. Green, M.I. Colado, *Psychopharmacology (Berl)* 154 (2001) 251.
13. R. Gollamudi, S.F. Ali, G. Lipe, G. Newport, P. Webb, M. Lopez, J.E. Leakey, M. Kolta, W. Slikker, *Neurotoxicology* 10 (1989) 455.
14. M. Segura, O. Jordi, M. Farré, J.A. McLure, M. Pujadas, N. Pizarro, A. Llebaria, J. Joglar, P.N. Roset, J. Segura, R. de la Torre, *Chem. Res. Toxicol.* 14 (2001) 1203.
15. D.C. Jones, C. Duvauchelle, A. Ikegami, C.M. Olsen, S.S. Lau, R. de la Torre, T.J. Monks, *J. Pharmacol. Exp. Ther.* 313 (2005) 422.
16. G.V. Erives, S.S. Lau, T.J. Monks, *J. Pharmacol. Exp. Ther.* 324 (2008) 284
17. C. Macedo, P.S. Branco, L.M. Ferreira, A.M. Lobo, J.P. Capela, E. Fernandes, M. de Lourdes Bastos, F. Carvalho, *J. Health Sci.* 53 (2007) 31.
18. D. Nematollahi, E. Tammari, *J. Org. Chem.* 70 (2005) 7769.
19. S. Shahroknian, M. Amiri, *Electrochem. Commun.* 7 (2005) 68.
20. F. Zhang, G. Dryhurst, *G. J. Electroanal. Chem.* 398 (1995) 117.
21. X.M. Shen, B. Xia, M.Z. Wrona, G. Dryhurst, *Chem. Res. Toxicol.* 9 (1996) 1117.
22. F. Zhang, G. Dryhurst, *J. Med. Chem.* 37 (1994) 1084.
23. R. Xu, X. Huang, K.J. Kramer, M.D. Hawley, *Bioorg. Chem.* 24 (1996) 110.
24. X.M. Shen, G. Dryhurst, *J. Med. Chem.* 39 (1996) 2018.
25. X. Huang, R. Xu, M.D. Hawley, T.L. Hopkins, K.J. Kramer, *Arch. Biochem. Biophys.* 352 (1998) 19.
26. M. Langeron, B. Lockhart, B. Pfeiffer, M.-B. Fleury, M.-B. *J. Med. Chem.* 42 (1999) 5043.
27. M. Langeron, M.B. Fleury, *J. Org. Chem.* 65 (2000) 8874.
28. M. Langeron, A. Neudörffer, M.B. Fleury, *Angew. Chem. Int. Ed.* 42 (2003) 1026.
29. E. Blattes, M.-B. Fleury, M. Langeron, *Electrochim. Acta* 50 (2005) 4902.
30. D. Xu, A. Chiaroni, M.-B. Fleury, M. Langeron, *J. Org. Chem.* 71 (2006) 6374.
31. A. Felim, A. Urios, A. Neudörffer, G. Herrera, M. Blanco, M. Langeron, *Chem. Res. Toxicol.* 20 (2007) 685.
32. R.J. Borgman, M.R. Baylor, J.J. McPhillips, R.E. Stitzel, *J. Med. Chem.* 17 (1974) 427.
33. P.H. Morgan, A.H. Beckett, *Tetrahedron* 31 (1975) 2595.

34. J.G. Cannon, Z. Perez, J.P. Long, D.B. Rusterholtz, J.R. Flynn, B. Costall, D.H. Fortune, R.J. Naylor, *J. Med. Chem.* 22 (1979) 901.
35. N. Milhazes, T. Cunha-Oliveira, P. Martins, J. Garrido, C. Oliveira, C.A. Rego, F. Borges, *Chem. Res. Toxicol.* 19 (2006) 1294.
36. F.P. Monnet, M.P. Morin-Surun, J. Leger, L. Combettes, *J. Pharmacol. Exp. Ther.* 307 (2003) 705.
37. J.K. Fallon, A.T. Kicman, J.A. Henry, P.J. Milligan, D.A. Cowan, A.J. Hutt, *Clin. Chem.* 45 (1999) 1058.
38. M.J. Morgan, *Neuropsychopharmacology* 19 (1998) 252.
39. E. O'Hearn, G. Battaglia, E.B. De Souza, M.J. Kuhar, M.E. Molliver, *J. Neurosci.* 8 (1988) 2788.
40. J.P. Capela, C. Macedo, P.S. Branco, L.M. Ferreira, A.M. Lobo, E. Fernandes, F. Remaio, M. L. Bastos, U. Dirnagl, A. Meisel, F. Carvalho, *Neurosciences* 146 (2007) 1743.